

Effects of Copolymer Sequence Distribution on the Miscibility of Poly(ethylene oxide)/Poly(styrene-*co*-acrylic acid) Blends: A Molecular Simulation Approach

Kyounghsei Choi and Won Ho Jo*

Department of Fiber and Polymer Science, Seoul National University, Seoul 151-742, Korea

Received September 21, 1995; Revised Manuscript Received September 10, 1996[®]

ABSTRACT: The effect of the copolymer sequence distribution on the miscibility of a poly(ethylene oxide) (PEO)/poly(styrene-*co*-acrylic acid) (SAA) blend has been investigated by molecular simulations. The molecular simulation provides a method to calculate the interaction energy parameter and hydrogen-bond energy. It is observed that both the sequence distribution and the composition of the SAA copolymer significantly affect the degree of miscibility. For a fixed composition, there exists an optimal range of sequence distributions for which the blend system is miscible.

Introduction

It is possible to obtain polymer blends of more desirable properties by mixing miscible polymers, and thus it is very important to examine the factors affecting the miscibility of polymer mixtures. The miscibility of homopolymer/copolymer blends has been successfully described by the binary interaction model.^{1–4} Based on the model, the effect of the composition of the copolymer on the miscibility of PEO/SAA blends was systematically investigated in our laboratory.⁵ It was suggested that both the specific interaction between ethylene oxide (EO) and acrylic acid (AA) segments and the intramolecular repulsive force in the SAA copolymer are responsible for the miscibility.

Progress in polymerization technology now allows control of the microstructural features of polymers such as tacticity. Experimental studies of the tacticity effect on polymer blend miscibility have been reported in some publications.^{6–9} It is reported that the tacticity of a polymer can affect the conformation of the chain, the probability of contact between interacting sites, and the interaction parameter, all of which will inevitably have an influence on miscibility. A theoretical approach to the tacticity effect has been initiated using an integral equation formalism,¹⁰ and the molecular origin of the tacticity effects on blend miscibility was examined.¹¹

The sequence distribution of the copolymer in homopolymer/copolymer blends will affect the charge distribution and the probability of contact between interaction sites, and consequently affect the miscibility of the blend. However, the binary interaction model is inadequate to study the sequence effect due to the assumption of a random distribution. Thus, Balazs *et al.*¹² developed a model describing the sequence effect on miscibility and showed that there is an optimal range of sequence distributions for which the homopolymer/copolymer system is miscible by using their own model.

In this paper, we analyze the effect of the copolymer sequence distribution in PEO/SAA blends by calculating the interaction energy parameters and the hydrogen-bond energy using molecular simulation methods.

Theoretical Background

For simplicity, we denote the monomeric units of AA, styrene, and EO as *a*, *b*, and *c* instead of using the full

names. The free energy of mixing for a binary mixture of a homopolymer and a copolymer, $c_{N_1}/(a_f b_{1-f})_{N_2}$, is given by^{1–3}

$$\frac{\Delta G}{RT} = \frac{\phi_1}{N_1} \ln \phi_1 + \frac{\phi_2}{N_2} \ln \phi_2 + \phi_1 \phi_2 \chi_{\text{tot}} \quad (1)$$

where χ_{tot} is the parameter that represents the strength of the polymer–polymer interaction. The homopolymer c_{N_1} has a volume fraction ϕ_1 and degree of polymerization N_1 , and the copolymer $(a_f b_{1-f})_{N_2}$ has a volume fraction ϕ_2 and degree of polymerization N_2 with the composition of *f* and $1 - f$. When the binary interaction model is invoked, the total interaction energy parameter χ_{tot} is given by

$$\chi_{\text{tot}} = f \chi_{ac} + (1 - f) \chi_{bc} - f(1 - f) \chi_{ab} \quad (2)$$

However, the simple binary interaction model is inadequate to study the sequence effects owing to its assumption of a random distribution. Assuming that the interaction energy parameters of all *a*–*a* and *b*–*b* pairs are equivalent and equal to zero and that all *a*–*b* interactions are equivalent to the average interaction parameter $\bar{\chi}_{ab}$, Balazs *et al.*¹² expressed χ_{tot} as the sum of the contribution of the composition χ_{comp} and the sequence distribution χ_{dist} as follows:

$$\chi_{\text{tot}} = \chi_{\text{comp}} + \chi_{\text{dist}} \quad (3)$$

$$\chi_{\text{comp}} = f_a \bar{\chi}_{ac} + f_b \bar{\chi}_{bc} - f_a f_b \bar{\chi}_{ab} \quad (4)$$

$$\chi_{\text{dist}} = \frac{f_{aa}^2}{f_a} \Delta \chi_a + \frac{f_{bb}^2}{f_b} \Delta \chi_b \quad (5)$$

where f_a and f_b are the fractions of *a* and *b* molecules in the copolymer, f_{aa} , f_{ab} , and f_{bb} are the pair probabilities of *aa*, *ab*, and *bb* pairs in a single chain, and thus $f_a = f_{aa} + f_{ab}$, $f_b = f_{bb} + f_{ab}$ and $f_{ab} = f_{ba}$. The $\bar{\chi}_{ac}$ is the average of the interactions between *a* occupying the central site in the triads and *c*, i.e., $\chi_{aaa:c}$, $\chi_{aab:c}$ and $\chi_{bab:c}$. The $\bar{\chi}_{bc}$ is similarly the average of $\chi_{aba:c}$, $\chi_{abb:c}$ and $\chi_{bbb:c}$. Although there are nine possible *a*–*b* interactions, all interactions will be assumed equivalent to the average interaction parameter $\bar{\chi}_{ab}$ which is the intramolecular interaction in the copolymer chain. Then, $\Delta \chi_a$ and $\Delta \chi_b$ are defined by eqs 6 and 7, respectively.

* To whom correspondence should be addressed.

© Abstract published in *Advance ACS Abstracts*, February 1, 1997.

$$\Delta\chi_a = \chi_{aaa:c} - \bar{\chi}_{ac} \quad (6)$$

$$\Delta\chi_b = \chi_{bbb:c} - \bar{\chi}_{bc} \quad (7)$$

A negative $\Delta\chi_a$ implies that *aaa-c* interactions are energetically more favorable than any other type of *a-c* interactions, and a similar comment is applicable to $\Delta\chi_b$. The parameters θ and δ are introduced to specify the sequence distribution and the composition, respectively.

$$\theta = \frac{f_{ab}}{2f_a f_b} \quad (8)$$

$$f_a = \frac{1}{2}(1 + \delta), \quad f_b = \frac{1}{2}(1 - \delta), \quad -1 \leq \delta \leq 1 \quad (9)$$

θ can range from 0 for a block copolymer to 1 for an alternating copolymer, with the value 0.5 for a random copolymer. For symmetric copolymers, $\delta = 0$, and the copolymer composition can be expressed by δ .

Model and Simulation

The Dreiding 2.21 force field¹³ was adopted for our simulations, and the Cerius² software from Molecular Simulations Inc. was used. The intramolecular interactions were described by force field terms including bond, bending, torsion, and inversion; the intermolecular interactions by terms including van der Waals, electrostatic, and hydrogen bonding.¹³

1. Validation of the Force Field. The Hildebrand solubility parameters of several homopolymers were calculated and compared to experimental data to examine the validity of the force field. The procedures to prepare an equilibrated structure are as follows. An atactic PS chain with 20 repeating units and a meso diad content of 50% was produced and then packed into a cubic simulation box with 3-D periodic boundaries. The size of the cubic box was chosen to correspond to the experimental density 1.05 g/cm³.¹⁴ At the first stage following generation of the initial structure in the simulation box, the energy of the structure was roughly minimized by the conjugate gradient method. Then, the structure was relaxed by performing NVT-molecular dynamics at 1000 K for 20 000 steps (1 step corresponds to 1 fs), followed by NVT-molecular dynamics at 300 K for 20 000 steps. To save computation time during rough equilibrations, the long-range nonbonded interactions were treated by cutting off the potential curve at 8.0 Å. This cutoff introduces discontinuities in the potentials and forces. Thus, a spline function¹⁵ was used to connect the potentials and forces over 8.0–8.5 Å to prevent the discontinuity. The structure was finally equilibrated by NVT-molecular dynamics at 300 K for 10 000 steps followed by energy minimization using conjugate gradients, where the Ewald method¹⁶ was used to calculate the nonbonded interactions.

The Hildebrand solubility parameter is the square root of the cohesive energy density, which is defined as the energy difference when a polymer of unit volume is evaporated in vacuum. Solubility parameters were obtained for five different equilibrated structures produced from initial configurations with different tacticity sequences but containing the same meso-diad fractions by following the standard method,¹⁷ where the energy of the bulk-state polymer was obtained using the Ewald method. The same procedures were applied to calculate the solubility parameters of PEO and poly(acrylic acid) (PAA), using densities of 1.128 and 1.045 g/cm³ for PEO

and PAA, respectively.^{14,21} The atactic PAA was modeled with a meso-diad fraction of 50%.

2. Determination of Miscibility. The procedures used in this study consist of two simulation methods. One is a so-called docking method¹⁸ combined with Balazs *et al.*'s theory,¹² and the other is molecular dynamics. The former is preferable to the latter, because the docking method requires much less computation time than the molecular dynamics does. Thus, our results mainly relied on the docking method to determine the miscibility of the blends, and molecular dynamics was only employed for obtaining additional subsidiary information on the contact probability between AA and EO.

Docking Methods. Docking methods can provide segmental interaction energy parameters.^{18,19} The interaction parameter χ_{ij} can be calculated from a knowledge of pairwise interactions, w_{kl} 's ($k, l \in \{i, j\}$), and coordination numbers, z_{kl} 's by using eq 10.

$$\chi_{ij} = \frac{1}{RT} \left(\frac{1}{2} (z_{ij} w_{ij} + z_{ji} w_{ji}) - \frac{1}{2} (z_{ii} w_{ii} + z_{jj} w_{jj}) \right) \quad (10)$$

where w_{kl} is an averaged pairwise interaction energy when a segment l is in contact with the center segment k . A similar explanation can be given for z_{kl} .

In order to simulate four w_{kl} 's and z_{kl} 's and to obtain χ_{ij} , the model segments i and j with proper charge distributions must be prepared. Nine model segments were prepared in this system: *aaa*, *aab*, *bab*, *aba*, *abb*, *bbb*, and *c* for the calculation of $\bar{\chi}_{ac}$ and $\bar{\chi}_{bc}$; *-a-* and *-b-* for the calculation of $\bar{\chi}_{ab}$. For the triads, the partial charges were calculated utilizing the charge equilibration method,²⁰ which is also available in the Cerius² software, after constructing and optimizing the triad structure, and then the monomeric units on both sides were removed. Thus, a monomer structure, which has the charge distribution of a monomer in the center of the triad, was prepared. For example, the structure of a triad *aba* was produced, the partial charges were calculated, and then *a*'s on both sides were removed, which produced a *b* segment with the charge distribution of the *b* monomer in the triad *aba*. The *b* segment will be denoted as *aba* in order to distinguish from other *b* segments which come from triads *abb* and *bbb*. The other model segments *aaa*, *aab*, *bab*, *abb*, and *bbb* were generated by following similar procedures. These segments of *a* and *b* were used for calculating $\bar{\chi}_{ac}$ and $\bar{\chi}_{bc}$. Additionally, the model segments *-a-*, *-b-*, and *c* were made to have the total charge of zero, where the model segments *-a-* and *-b-* were prepared for calculating $\bar{\chi}_{ab}$. As mentioned above, all the *a-b* interactions in the copolymer chains were assumed to be equivalent to the average interaction parameter $\bar{\chi}_{ab}$ to reduce the number of interaction energy terms, and thus the model segments *-a-* and *-b-* were produced separately from the other model segments.

No segments are allowed to make contact in the chain direction due to the chain connectivity. Thus, all segments were made inaccessible on both sides in the chain direction by introducing two dummy atoms at the head and tail positions of the segments, which prevented contacts with other atoms.

A particular configuration of segments i and j was produced with them touching each other, and the pairwise interaction energy for the configuration was calculated. The same procedure was repeated 100 000 times, and the Metropolis criterion was used to determine whether to accept these configurations at a certain

Table 1. Hildebrand Solubility Parameters in (MPa)^{1/2}

polymer	density	solubility parameters						exptl ^a
		sample 1	sample 2	sample 3	sample 4	sample 5	average	
PS (<i>at.</i>)	1.050 ^a	16.5	17.4	17.7	17.3	16.8	17.1 ± 0.4	17.52
PEO	1.128 ^a	20.4	23.7	18.1	23.8	22.5	21.7 ± 2.2	20.2 ± 2
PAA (<i>at.</i>)	1.045 ^b	18.1	17.3	19.3	19.7	19.8	18.8 ± 1.0	18.0

^a From ref 14 ^b From ref 21.

temperature. The interaction energy $w_{kl}(T)$ was determined by averaging the energies of all accepted configurations at a given temperature. The coordination numbers z_{kl} 's were obtained by calculating and averaging the possible numbers of nearest neighbors (l) in contact with the center segment (k) over 500 trials. More detailed explanations can be found elsewhere.¹⁸

Molecular Dynamics. Another approach, molecular dynamics combined with molecular mechanics, can in principle provide more exact information on the pairwise energy. However, this method requires very long computing times and also yields interaction energies that depend strongly upon the initial configuration of polymers. Furthermore, strong specific interactions such as hydrogen bonding can prevent chains from relaxing, making it difficult to generate equilibrium structures. Therefore, many samples and error analysis are essential to obtain meaningful results. Hydrogen-bond energies were calculated for PEO/SAA blends, in which the SAA chain is either a random or a block copolymer, to estimate the effect of local chain conformations on the interaction energy parameters. The primary box contains an SAA chain of 100-mers and four PEO chains of 25-mers. Instead of one long PEO chain, four short PEO chains were employed to yield a higher probability of interchain contact. Eight to twelve samples were prepared with initially random torsional angles and then relaxed by molecular mechanics. The structures were annealed at high temperature by NVT-molecular dynamics without turning on the strong specific interactions such as electrostatic and hydrogen-bond energies, to prevent early fixation of the structures and to ensure easy relaxation of the chains. Then, the structures were relaxed again at room temperature by NVT-molecular dynamics. After equilibration, molecular dynamics was performed using the microcanonical ensemble, and the hydrogen-bond energies were calculated. The density was fixed at 1.0 g/cm³ for all the systems.

Results and Discussion

The simulated solubility parameters of homopolymers are listed in Table 1. The simulated results agree well with the experimental values, although the values have some scattering which may arise from both small number of samples and relatively short chain. This suggests that the Dreiding 2.21 force field is adequate for PS, PEO, and PAA.

Total charge values for the segments *aaa*, *aab*, and *bab* produced by the charge equilibration method are -0.009, -0.111, and -0.204, respectively. It is recalled that the total charge values of the segments *aaa*, *aab*, and *bab* correspond to those of the center monomer (*a*) only in each triad. The electron density in *a* increases with the substitution of *b* which donates electrons more readily than *a*. Total charge values of the segments *aba*, *abb*, and *bbb* are 0.181, 0.028, and 0.032. This means that a monomer *b* connected to the electron-withdrawing monomer *a* as its neighbor has a more positive net

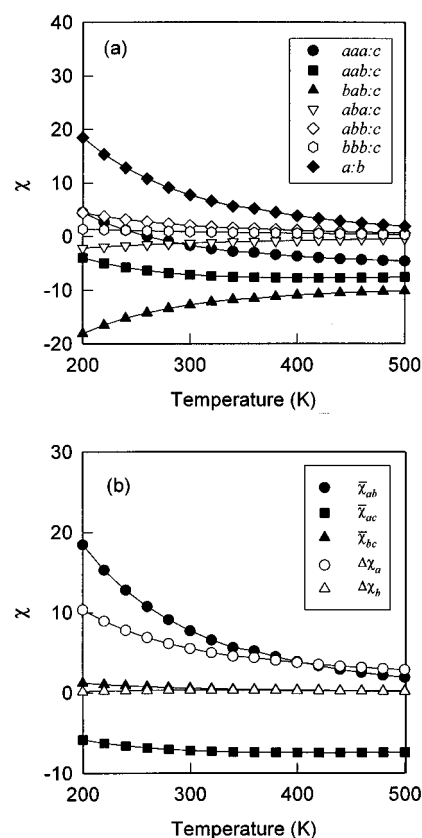


Figure 1. (a) Interaction energy parameters as a function of temperature obtained by molecular simulations. (b) The interaction energy parameters which are calculated from those in (a). The meaning of the notations in the inset is explained in the text.

charge than when next to a *b*. Total charge values of the other model segments, *-a-*, *-b-*, and *c* are zero.

The interaction energy parameters were calculated for the model segments which have proper charge distributions by the docking method. Figure 1a shows that the interaction between *a* and *c* is favorable, especially when *a* is activated by *b* which donates electrons to its covalent-bonded neighbors. It is noteworthy that the interaction between the sequence *aaa* and *c* is relatively unfavorable, which results in a positive $\Delta\chi_a$. This means that blockiness of *a* may lead to a negative contribution to miscibility. The experimental results showed that there exist both a specific interaction between *a* and *c* and an intramolecular repulsion between *a* and *b*.⁵ The experimental trends are seen in Figure 1b, where $\bar{\chi}_{ab}$ is seen to be strongly positive whereas $\bar{\chi}_{ac}$ has a strongly negative value. Balazs *et al.*¹² assumed that $\bar{\chi}_{ac} = \chi_{aab:c} = \chi_{baa:c} = \chi_{bab:c} \neq \chi_{aaa:c}$ and $\bar{\chi}_{bc} = \chi_{abb:c} = \chi_{bba:c} = \chi_{aba:c} \neq \chi_{bbb:c}$ to reduce the number of interaction terms. However, in the present study, all the interaction terms such as $\chi_{aab:c}$ ($=\chi_{baa:c}$), $\chi_{bab:c}$, $\chi_{aaa:c}$, $\chi_{abb:c}$ ($=\chi_{bba:c}$), $\chi_{aba:c}$, and $\chi_{bbb:c}$ were calculated, and $\bar{\chi}_{ac}$ and $\bar{\chi}_{bc}$ were taken as average values of corresponding triads, because it is unreasonable to assume $\chi_{aab:c} = \chi_{bab:c}$ and $\chi_{abb:c} = \chi_{aba:c}$ as one sees from

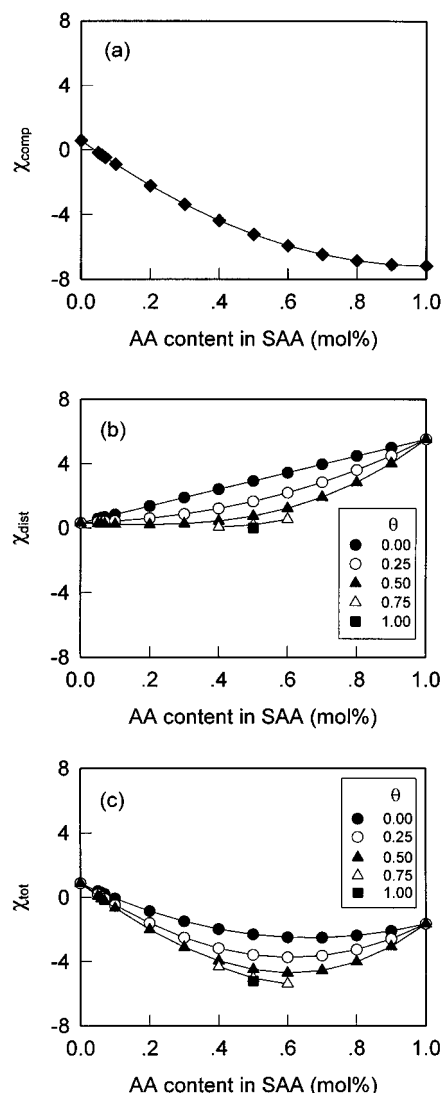


Figure 2. Interaction energy parameters at room temperature obtained by combining molecular simulations and the theory of Balazs *et al.*: (a) the composition dependent interaction energy parameter χ_{comp} ; (b) the sequence distribution dependent interaction energy parameter χ_{dist} ; (c) the total interaction energy parameter χ_{tot} .

Figure 1a. Cantow *et al.*²² also criticized Balazs *et al.*'s assumption. They asserted that the assumption causes some inconsistency. They redefined $\Delta\chi_a$ and $\Delta\chi_b$ as $\Delta\chi_a = \chi_{aaa:c} - \chi_{aab:c} = \chi_{aab:c} - \chi_{bab:c}$ and $\Delta\chi_b = \chi_{bbb:c} - \chi_{bba:c} = \chi_{bba:c} - \chi_{aba:c}$. Figure 1 shows $\chi_{aab:c} \approx \bar{\chi}_{ac}$ and $\chi_{aaa:c} - \chi_{aab:c} \approx \chi_{aab:c} - \chi_{bab:c}$ at above room temperature, and thus our $\Delta\chi_a$ has almost the same value as the $\Delta\chi_a$ obtained using the definition of Cantow *et al.* In the case of $\Delta\chi_b$, the situation is not the same as $\Delta\chi_a$, but the $\Delta\chi_b$ has too small a value compared with $\Delta\chi_a$ to affect χ_{dist} . Consequently, our simulation results for χ_{dist} are well consistent with those obtained from the definition of Cantow *et al.*

The total interaction energy parameter χ_{tot} , the composition dependent component χ_{comp} , and the sequence distribution dependent component χ_{dist} were obtained by incorporating the simulated interaction parameters into eqs 3–5. The monomer fractions (f_a and f_b) and diad fraction (f_{ab}) were determined by varying θ and δ in eqs 8 and 9. An increase of AA content in SAA produces more AA–EO interactions, which is favorable for miscibility and thus leads to a negative χ_{comp} (Figure 2a). In the limit that the composition of AA approaches

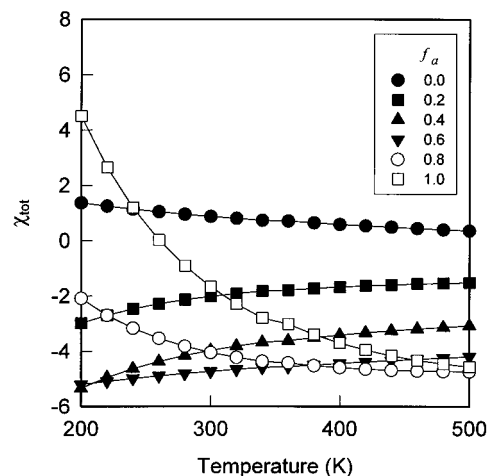


Figure 3. Total interaction energy parameters as a function of temperature for $\theta = 0.5$.

1.0, χ_{dist} becomes equal to $\Delta\chi_a$. In the other limit that the composition of AA approaches 0.0, χ_{dist} becomes equal to $\Delta\chi_b$. Because $\Delta\chi_a$ is larger than $\Delta\chi_b$, χ_{dist} increases with the AA content (Figure 2b). The blockiness of the sequence represented by lower θ has a negative effect on the miscibility, which seems to arise from the strong tendency of $\chi_{aaa:c} > \chi_{aab:c} > \chi_{bab:c}$ as shown in Figure 1a. As a result, the PEO is more miscible with the SAA copolymer having an alternating sequence (Figure 2c). The maximum value of θ is limited by the composition:

$$\theta_{\text{max}} = \frac{1}{1 + \delta} \quad (11)$$

In the case of a symmetric copolymer (*i.e.* $\delta = 0$), θ_{max} equals unity such that the copolymer can have sequence distributions ranging from block to alternating.

The temperature dependence of the total interaction parameter shows that there exists an optimum condition for the composition at a given temperature (Figure 3). Binary blends of PEO/PS and PEO/PAA are immiscible and miscible, respectively, at room temperature. The shape of curves implies that the homopolymer/homopolymer blends will exhibit UCST (upper critical solution temperature) behaviors.

A drastic effect of the sequence distribution on the miscibility can be found in Figure 4. As the AA content in SAA increases from 5 mol % (Figure 4a) to 7 mol % (Figure 4b) to 10 mol % (Figure 4c), the blend becomes more miscible. The blend with random copolymers becomes miscible at a composition between 5 and 7 mol %, which agrees well with the experimental results.⁵ At 7 mol %, the blend with block copolymers shows positive χ_{tot} , while the blend with random copolymers has negative χ_{tot} . This is very interesting because the miscibility could be controlled only by the change of copolymer sequence distributions.

The difference in the spatial distribution of interaction sites may also affect the effective interaction. The theory adopted here, however, does not accommodate the physical aspects of chain conformations, and thus the probability of contacts between segments only based on the mean field approximation is considered. In our simulation, the information on the probability of contacts could be obtained by calculating hydrogen-bond energy, because the number of contacts is proportional to the hydrogen-bond energy. The intermolecular hydrogen-bond energy between AA and EO (Figure 5d)

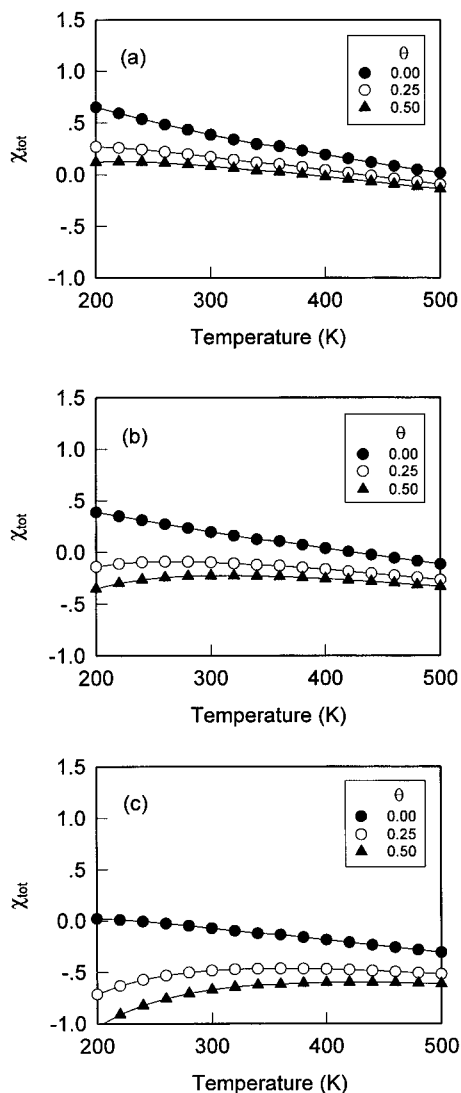


Figure 4. Total interaction energy parameter between PEO and SAA for (a) 5, (b) 7, and (c) 10 mol % of AA in SAA.

was obtained by subtracting the intramolecular hydrogen-bond energies (Figure 5b and 5c) from the total hydrogen-bond energy (Figure 5a). When the AA content is small, AA segments in random copolymers which have more sparse distribution will have fewer chances to meet EO segments because AA's are buried in styrene segments and thus the intermolecular interactions are prevented. When the AA content is large, the self-association of intramolecular AA's in the block copolymer rapidly increases, which prevents the formation of the intermolecular hydrogen bond. Consequently, there exists a competition between self-associations of AA's and intermolecular hydrogen bonds of EO-AA pairs, and the competition is a function of the composition and the sequence distribution. However, the hydrogen-bond energies which reflect the local spatial distribution of interaction sites do not vary as much as the total interaction with the sequence distribution as shown in Figure 5. The total interaction between AA and EO can be calculated from eq 12:

$$\chi_{\text{total},ac} = \frac{f_{ab}^2}{f_a} \chi_{bab:c} + 2 \frac{f_{ba} f_{aa}}{f_a} \chi_{baa:c} + \frac{f_{aa}^2}{f_a} \chi_{aaa:c} \quad (12)$$

The results show the difference of about 600–1000% in the total interaction energies for block and random

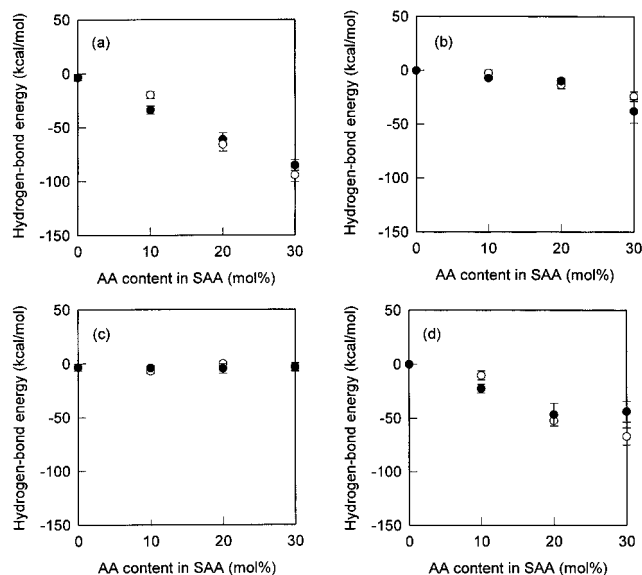


Figure 5. Hydrogen-bond energy calculated by molecular dynamics and molecular mechanics: (a) total; (b) self-association between AA segments; (c) self-association between EO segments; (d) interchain hydrogen bond between AA and EO segments. Filled and open circles represent block and random copolymer, respectively.

copolymers, whereas the differences of hydrogen bond energies are of about 20–40%. Therefore, the contribution of the local spatial distribution of the interaction sites to the interaction energy is relatively small compared to the segmental interaction itself. One can conclude that it is not necessary to incorporate the contribution of the local spatial distribution into the determination of miscibility for PEO/SAA blends. In other words, the interaction energy parameters need not be scaled by the ratios of contact probabilities arising from the local spatial distribution, which means Balazs *et al.*'s original theory is sufficient to estimate the miscibility of PEO/SAA blends. This is why more extensive molecular dynamics with more refined densities for the calculation of hydrogen bond has not been conducted.

As a virtual experiment performed on computers, molecular simulation methods can provide helpful information to understand the physical nature in a qualitative sense and may often give quantitative predictions, although it is not always possible to compare all the simulated results with the real experimental ones at this time. It is noteworthy that the effect of sequence distribution on phase behaviors can be approached in different ways. Recently, extensive research efforts have been devoted to models where the effect of the sequence distribution manifests itself only in the number of different segment–segment interactions.^{23–25} However, their models have not been examined in this study.

Conclusions

Molecular simulations were carried out to study the effect of sequence distribution of copolymer on the miscibility of PEO/SAA blends by calculating the interaction energy parameters and hydrogen-bond energy. It is observed that both the composition and the sequence distribution significantly affect the degree of miscibility. For a fixed composition, there exists an optimal range of sequence distribution for which the blend system is miscible. The sequence distribution

does not only affect the charge distribution of segments which in turn affects the contact energy, but also affects the probability of contacts between interaction sites. It is also observed that the segmental interaction energy itself is more important than the local spatial distribution of the segments, to determine the effect of the copolymer sequence distribution on the miscibility. There exists a competition between self-associations of AA's and intermolecular hydrogen bonds of EO-AA pairs, and the competition is a function of the composition and the sequence distribution.

Acknowledgment. The authors thank Cheil Industries Inc. for their financial support.

References and Notes

- (1) ten Brinke, G.; Karasz, F. E.; MacKnight, W. J. *Macromolecules* **1983**, *16*, 1827.
- (2) Paul, D. R.; Barlow, J. W. *Polymer* **1984**, *25*, 487.
- (3) Kambour, R. P.; Bendler, J. T.; Bopp, R. C. *Macromolecules* **1983**, *16*, 753.
- (4) Roe, R. J.; Rigby, D. In *Advances in Polymer Science* 82; Springer-Verlag: Berlin, 1987.
- (5) Jo, W. H.; Lee, S. C. *Macromolecules* **1990**, *23*, 2261.
- (6) Schurer, J. W.; de Boer, A.; Challa, G. *Polymer* **1975**, *16*, 201.
- (7) Lemieux, E.; Prud'homme, R. E.; Forte, R.; Jerome, R.; Teyssie, P. *Macromolecules* **1988**, *21*, 2148.
- (8) Beaucage, G.; Stein, R. S.; Hashimoto, T.; Hasegawa, H. *Macromolecules* **1991**, *24*, 3443.
- (9) Beaucage, G.; Stein, R. S. *Macromolecules* **1993**, *26*, 1609.
- (10) Schweizer, K. S.; Curro, J. G. In *Advances in Polymer Science* 116; Springer-Verlag: Berlin, 1994.
- (11) Honeycutt, J. D. *Makromol. Chem., Macromol. Symp.* **1993**, *65*, 49.
- (12) Balazs, A. C.; Sanchez, I. C.; Epstein, I. R.; Karasz, F. E.; MacKnight, W. J. *Macromolecules* **1985**, *18*, 2188.
- (13) Mayo, S. L.; Olafson, B. D.; Goddard, W. A., III. *J. Phys. Chem.* **1990**, *94*, 8897.
- (14) Brandrup, J.; Immergut, E. H., Eds. *Polymer Handbook*, 3rd Ed.; John Wiley & Sons: New York, 1989.
- (15) Cerius² version 1.6 Simulation Tools User's Reference, Molecular Simulations Inc.; Press, W. H., et al. *Numerical Recipes in C*, 2nd Ed.; Cambridge University Press: Cambridge, 1992.
- (16) De Leeuw, S. W.; Perram, J. W.; Smith, E. R. *Proc. R. Soc. London* **1980**, *A373*, 27.
- (17) Theodorou, D. N.; Suter, U. W. *Macromolecules* **1985**, *18*, 1467.
- (18) Fan, C. F.; Olafson, B. D.; Blanco, M.; Hsu, S. L. *Macromolecules* **1992**, *25*, 3667.
- (19) Tao, H.-J.; Fan, C. F.; MacKnight, W. J.; Hsu, S. L. *Macromolecules* **1994**, *27*, 1720.
- (20) Rappé, A. K.; Goddard, W. A., III. *J. Phys. Chem.* **1991**, *95*, 3358.
- (21) Mark, H. F., et al., Eds. *Encyclopedia of Polymer Science and Engineering*, 2nd Ed.; John Wiley & Sons: New York, 1989; Vol. 1.
- (22) Cantow, H.-J.; Schulz, O. *Polym. Bull.* **1986**, *15*, 449.
- (23) Fredrickson, G. H.; Milner, S. T.; Leibler, L. *Macromolecules* **1992**, *25*, 6341.
- (24) Angerman, H.; Hadzioannou, G.; ten Brinke, G. *Phys. Rev. E* **1994**, *50*, 3808.
- (25) Sfatos, C. D.; Gutin, A. M.; Shakhnovich, E. I. *Phys. Rev. E* **1995**, *51*, 4727.

MA951421H